Negative quasiclassical magnetoresistance in a high density two-dimensional electron gas in a $Al_xGa_{1-x}N/GaN$ heterostructure

Hyun-Ick Cho
Kyungpook National University, 1370, Sankyuk-Dong, Daegu 702-701, Korea

G. M. Gusev
Instituto de Física da Universidade de São Paulo, CP 66318, CEP 05315-970, São Paulo, Brazil

Z. D. Kvon
Institute of Semiconductor Physics, Novosibirsk, Russia

V. T. Renard
GHMFL, BP-166, F-38042, Grenoble, Cedex 9, France, INSA-Toulouse, 31077, Cedex 4, France

Jung-Hee Lee
Kyungpook National University, 1370, Sankyuk-Dong, Daegu C.P.702-701, Korea

J-C. Portal
GHMFL, BP-166, F-38042, Grenoble, Cedex 9, France, INSA-Toulouse, 31077, Cedex 4, France and Institut Universitaire de France, Toulouse, France

(Received 12 January 2005; published 24 June 2005)

We studied the negative temperature-independent magnetoresistance in a high-density, two-dimensional electron gas in $Al_xGa_{1-x}N/GaN$ heterostructure. This magnetoresistance is attributed to the classical percolation of electrons in a random array of strong scatterers (interface roughness) on the background of the smooth impurity potential. The ratio between the mean free paths due to strong scatterers and smooth disorder was deduced from the comparison of the data and the theory. Independently, the roughness scattering has been measured and calculated using the roughness parameters. Therefore, the negative magnetoresistance in combination with the zero field mobility and Shubnikov–de Haas oscillations analysis allowed us to obtain information about long-range and short-range scattering mechanisms in $Al_xGa_{1-x}N/GaN$ heterostructure.

DOI: 10.1103/PhysRevB.71.245323 PACS number(s): 73.23.Ad, 72.10.−d, 72.20.Dp, 73.50.Bk

I. INTRODUCTION

New theoretical models[1–3] have refocused attention on the quasiclassical magnetotransport properties of a two-dimensional electron gas. Within the quasiclassical Lorentz approach it has been predicted that systems with a long-range component of disorder and dilute large size scatterers (hard disks) should exhibit a negative magnetoresistance (MR). This result disagrees with the Drude-Boltzmann model, which is equivalent to a stochastic redistribution of all scatterers after each collision and predicts zero magnetoresistance. The Lorentz-Boltzmann approach includes a more rich physics because it takes into account that a fraction P of the electrons in the two-dimensional (2D) system remains in collisionless cyclotron orbit forever. Their fraction is given by the formula[1,4,5]

$$P = \exp\left(-\frac{2\pi R_c}{l_s}\right) = \exp\left(-\frac{2\pi}{\beta}\right), \tag{1}$$

where $R_c = v_F/\omega_c$ is the cyclotron radius, v_F is the Fermi velocity, $\omega_c = eB/mc$ is the cyclotron frequency, m is the effective mass, $\beta = l_s/R_c, l_s = 1/(2Nd)$ is the transport mean free path, N is the disk density, and d is the effective diameter of the disks. Such circling electrons do not contribute to the conductivity σ_{xx}; however, they give a nonzero contribution to σ_{xy}. The conductivity of the rest of the "wandering" electrons, which collide with the disks, can be described by the conventional Drude expressions

$$\sigma_{xx} = \frac{\sigma_0}{1+\beta^2}, \quad \sigma_{xy} = \frac{\sigma_0\beta}{1+\beta^2}, \tag{2}$$

where $\sigma_0 = n_s e^2 \tau_{tr}/m$ is the zero field conductivity, n_s is the electron density, τ_{tr} is the momentum relaxation time. Finally, the contributions of both "circling" and wandering electrons results in the following resistivity tensor:[5]

$$\rho_{xx} = \rho_0 \frac{1-P}{1+P^2/\beta^2}, \quad \rho_{xy} = \rho_0\beta\frac{1-P^2/\beta^2}{1+P^2/\beta^2}, \tag{3}$$

where $\rho_0 = 1/\sigma_0$ is the zero-field resistivity. We see that this equation predicts a negative magnetoresistance.

It is worth noting that real 2D electron gases in $Al_xGa_{1-x}As/GaAs$ heterostructures show a B-independent magnetoresistance in low magnetic field; therefore, the transport in high-mobility 2D systems is more relevant to the classical Drude-Boltzmann model than to the Lorentz-Boltzmann approach. Only recently has a classical 2D Lorentz gas been realized in an $Al_xGa_{1-x}As/GaAs$ heterostruc-

ture with a disordered array of antidots.[6,7] Surprisingly, a linear negative magnetoresistance has been found[7] instead of the parabolic negative magnetoresistance predicted by Eq. (3). Naively, such observation disagrees with the Lorentz-Boltzmann description. However, Refs. 8 and 9 demonstrated that the Lorentz-Boltzmann approach is in fact much richer than expected. In principle the behavior of the wandering electrons is described by the Drude model except for the recollision processes. Such recollisions introduce memory effects into the system and turn out to be very important. For example, in strong magnetic fields the electron recollides with the same antidot and forms rosettelike trajectories. This effect leads to the localization of electrons in magnetic fields $\omega_c > \omega_{perc} = 1.67 v_F N^{1/2}$. In low magnetic fields memory effects result in low angle return events to a scatterer (1) after a single collision process with another scatterer (2). Such non-Marcovian processes have been considered in Ref. 5. The theory predicts a linear negative magnetoresistance and explains the results obtained in random arrays of antidots.[6,7] Equation (4) summarizes the asymptotic behavior of the negative magnetoresistance (NMR) in a wider range of magnetic fields[9]

$$\frac{\Delta\rho_{xx}(B)}{\rho_{xx}(0)} = -\beta_0 \begin{cases} 0.33z^2 & \text{for } z \lesssim 0.05 \\ 0.032(z-0.04) & \text{for } 0.05 \lesssim z \lesssim 2 \\ 0.39 - 1.3z^{-1/2} & \text{for } z \to \infty \end{cases}, \tag{4}$$

where $z = \beta/\beta_0, \beta_0 = d/l_s = 2Nd^2$. Very recently a large linear NMR has been observed in $Al_xGa_{1-x}As/GaAs$ corrugated heterostructures.[10] These measurements also confirmed that the NMR is parabolic close to zero magnetic field for $z < 0.05$.

Real systems may show a combination of different types of disorder. In Ref. 11 a two-component model of disorder has been considered: a random array of rare strong scatterers (antidots, interface roughness) on the background of a smooth random potential (remote impurities). This model predicts a negative parabolic magnetoresistance

$$\frac{\Delta\rho_{xx}(B)}{\rho_{xx}(0)} \simeq -(\omega_c/\omega_0)^2, \tag{5}$$

where $\omega_0 = (2\pi N)^{1/2} v_F (2\gamma l_s/l_L)^{1/4}, l_L = v_F \tau_L$ is the transport mean free path due to the scattering by the smooth random potential, $\gamma \sim 1$.

The negative parabolic classical magnetoresistance has been observed recently in narrow GaAs wells with self-organized nonplanar heterointerfaces.[12] However, in these structures $l_s \sim l_L$ and one cannot consider them as a dilute array of strong scatterers. Therefore comparison with the theory which considers this case is difficult. However, this study demonstrated the importance of memory effects.

The transport properties of a 2D electron gas in an $Al_xGa_{1-x}N/GaN$ heterostructure have been intensively investigated due to the extraordinary importance of III-nitride optical and electrical devices.[13] Recently, the quality of such structures has been improved dramatically.[14] In this work we present the study of the negative magnetoresistance in a high-density, two-dimensional electron gas in an $Al_xGa_{1-x}N/GaN$ heterostructure. The magnetoresistance is analyzed in terms of the two component of disorder model,[11] and we show that this analysis allows determination of the properties of 2D electron gas. Therefore, in combination with other methods (Shubnikov–de Haas oscillations, zero-field mobility), it can be used to determine the scattering time due to the short and long-range scattering potentials.

II. EXPERIMENT

We measured high-density 2D electron gas in an $Al_xGa_{1-x}N/GaN$ heterostructure grown by metal-organic chemical vapor deposition (MOCVD) on a C(0001)-plane sapphire substrate with different thickness of the $Al_xGa_{1-x}N$ layer (30, 50, and 100 nm). Undoped GaN buffer layer with thickness of 330 Å,which was grown under 300 torr at 550 °C,is followed by undoped GaN ($\sim$2.5 μm), which was grown under 300 torr at 1020 °C. The undoped $Al_{0.3}Ga_{0.7}N$ barrier was grown under 50 torr at 1050 °C. The barrier thickness was 300, 500, and 1000 Å for samples KNU01, KNU02, and KNU03, respectively. After the growth, standard Hall bars were fabricated to carry out magneto-transport measurements. The samples with a 30 and 50 nm $Al_xGa_{1-x}N$ layer showed the following parameters: and $n_s = (1.1\text{–}1.2) \times 10^{13}$ cm^{-2}; the samples with a 100 nm $Al_{0.3}Ga_{0.7}N$ layer have $\mu \approx 4000$ cm^2/Vs and $n_s = 1.1 \times 10^{13}$ cm^{-2}. The test samples were Hall bars, with the distance between the voltage probes $L = 200$ μm and the width of the bar $d = 100$ μm. Four terminal resistance R_{xx} and Hall R_{xy} measurements were made down to 1.5 K in a magnetic field up to 15 T. The resistance $R_{xx}(B)$ is determined by integrals over the local resistivity tensors

$$R_{xx}(B) = \rho_{xx} \frac{\int J_x(x,y)dx + \tan(\theta_H) \int J_y(x,y)dx}{\int J_x(x,y)dy}, \tag{6}$$

where $\Theta_H = \tan^{-1}(\rho_{xy}/\rho_{xx})$ is the Hall angle, J_x, J_y are current densities in the x and y directions. The probe contacts are far from the ends of the Hall bar (in our samples the length to width ratio is 6), and we have a homogeneous current flow with $J_x = \text{const}$ and $J_y = 0$, resulting in $R_{xx} = \rho_{xx}(L/W)$ for any Hall angle.

The surface morphology of the samples has been measured by atomic force microscope. We have measured both the profile of the GaN surface before growth of the $Al_{0.3}Ga_{0.7}N$ material, and $Al_{0.3}Ga_{0.7}N$ surface profile after the growth. Since the results are coincident, we believe that the structure's surface accords with roughness of the quantum well. We compared the profile of the $Al_{0.3}Ga_{0.7}N/GaN$ interface obtained from 4×4 μm^2 scans with the correlator $<\Delta(r)\Delta(r)> = \Delta^2 \exp[-(r-r)^2/\Lambda^2]$, and deduced the roughness amplitude Δ and the lateral correlation scale of the roughness Λ. Figure 1 shows the atomic force microscope images and profiles of the $Al_{0.3}Ga_{0.7}N/GaN$ interface for the sample KNU01. A summary of the sample parameters is given in Table. I

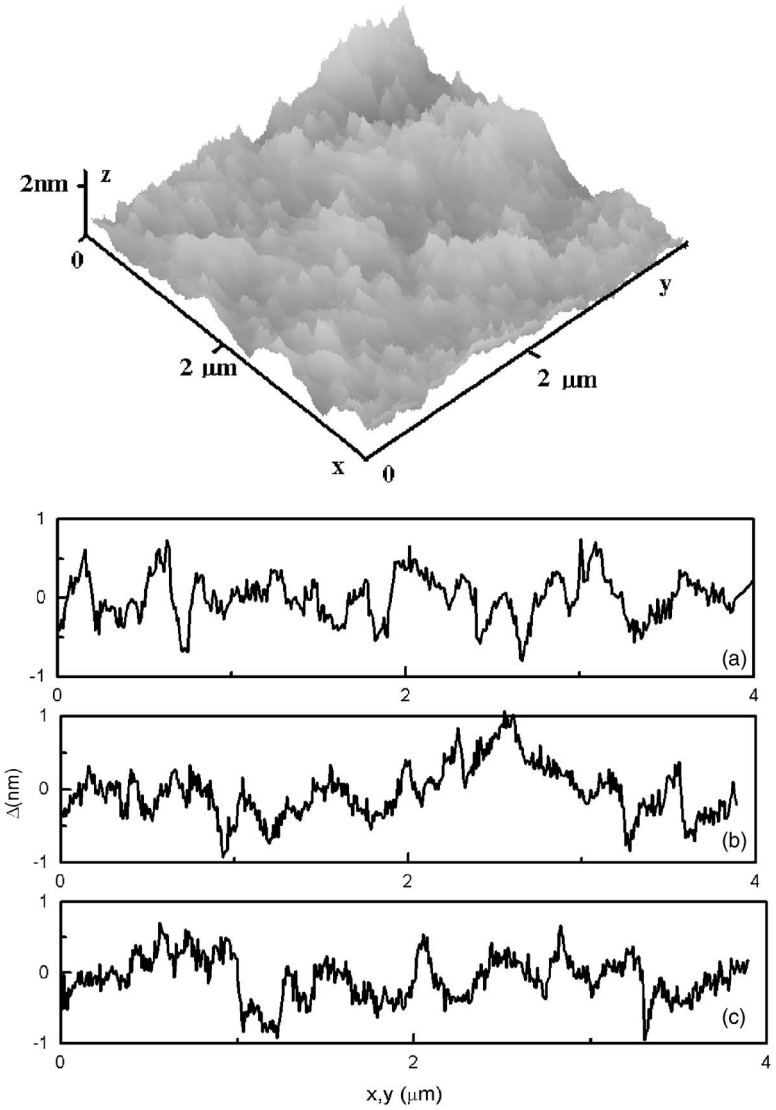

FIG. 1. Top: AFM image of the $Al_xGa_{1-x}N/GaN$ surface of a sample KNU01. (a), (b), and (c) Surface profiles across the different regions of the sample.

Figure 2 shows the longitudinal resistance R_{xx} for three different samples. A negative magnetoresistance followed by Shubnikov–de Haas oscillations is observed. It is worth noting that this NMR is a general characteristic of high-density, low-mobility 2D gases in GaN systems. See, for example, Fig. 1 in Ref. 15 and Fig. 1 in Ref. 16; in these studies the measured samples had similar electronic properties and show similar parabolic NMR. To our knowledge, this NMR has not been analyzed yet. Below a detailed comparison with recent theoretical models[5,9,11] is presented. We also focus on the results obtained in sample KNU01. Other samples have identical parameters and demonstrate similar behavior.

III. SCATTERING LIFETIMES DUE TO INTERFACE ROUGHNESS

Before analyzing the magnetoresistance, one should determine which is the main scattering mechanism in

TABLE I. The sample parameters. W is the thickness of the $Al_xGa_{1-x}N$ layer. Δ and Λ are roughness height and correlation length of the roughness, respectively. n_s is the electron density, μ is the zero-field mobility. τ_{tr} is the transport scattering time, and τ_q is the single particle relaxation time or quantum time. l_s/l_L is the ratio between the transport mean free path due to the scattering by the roughness and smooth random potential, determined from the parabolic negative magnetoresistance (see the text).

Sample	Substrate	W (xÅ)	n_s (10^{13} cm^{-2})	μ (cm^2/Vs)	τ_{tr} (ps)	τ_q (ps)	Δ (Å)	Λ (Å)	l_s/l_L
KNU01	Sapphire	300	1.1	4040	0.5	0.038	4.2	120	2.8
KNU02	Sapphire	500	1.2	4400	0.55	0.042	4.5	130	2.8
KNU03	Sapphire	1000	1.1	4280	0.54	0.042	4.5	110	2.5

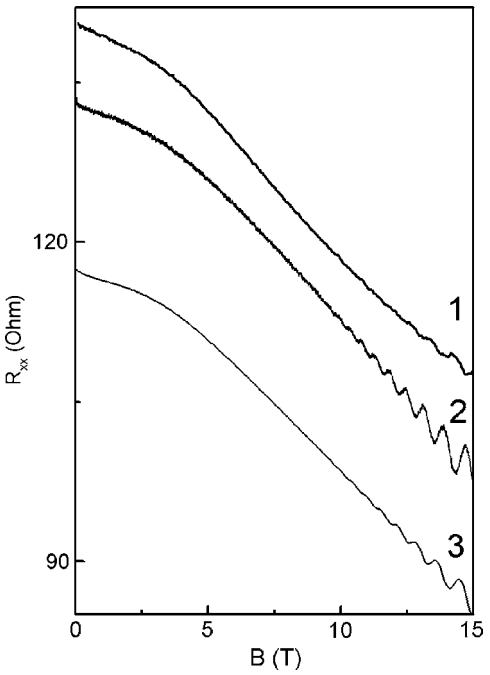

FIG. 2. The magnetoresistance as a function of magnetic field for different samples (1) KNU01 ($T=1.7$ K), (2) KNU03 ($T=1.5$ K), (3) KNU02 ($T=1.7$ K).

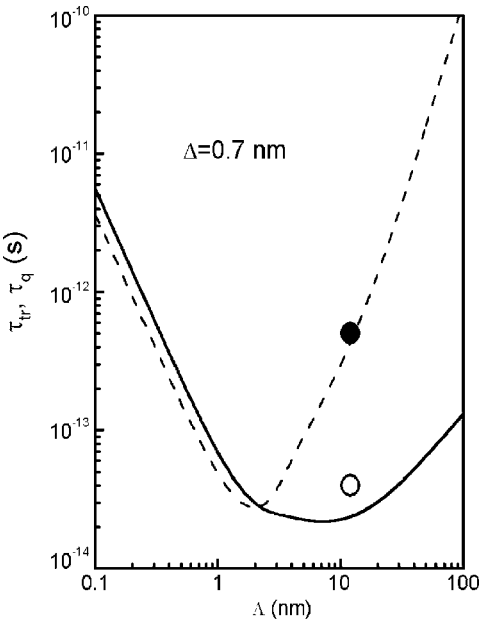

FIG. 3. Transport (solid line) and quantum (dashed line) scattering times due to the roughness scattering calculated using Eqs. (7)–(9) as a function of the correlation length. Circles are measured transport (empty dot) and quantum (full dot) scattering times for sample KNU01.

$Al_xGa_{1-x}N/GaN$ samples in order to use the relevant theory to analyze the data.

It has been shown Ref. 16 that the measured mobility decreases with the electron density at $n_s > 4.7\times10^{12}$ cm^{-2}. Such effect is consistent with interface roughness scattering.[18] The ratio between the transport scattering time τ_{tr} and the single particle relaxation time or quantum time τ_q can also give information about the main scattering mechanism. Short-range scattering processes (such as alloy or phonons scattering) result in a ratio τ_{tr}/τ_q close to the one, in contrast with interface roughness or Coulomb scattering, which may enhance this ratio by several orders in magnitude.[18] The transport time can be derived from the zero-field mobility $\mu=e\tau_{tr}/m$, and the quantum time is usually determined from the amplitude of the Shubnikov–de Haas (SdH) oscillations, which is given by the Lifshic-Kocevich formula

$$\frac{\Delta\rho_{xx}(B)}{\rho_{xx}(0)} = A\frac{4X}{\mathrm{Sinh}\,X}\exp\left(-\frac{\pi}{\omega_c\tau_q}\right)\cos\left(\frac{2\pi^2\hbar n_s}{eB}\right), \quad (7)$$

where $X=2\pi^2kT/\hbar\omega_c$, A is a numerical coefficient in the order of unity.

The quantum time was deduced from the comparison of the experimental curves to Eq. (7). We found a large ratio between transport and quantum scattering times in our structure ($\sim$10; see Table I). This is consistent with previous measurements[15–17] of the transport properties of a low-mobility, high-density $Al_xGa_{1-x}N/GaN$ heterostructure and with the fact that interface roughness plays a significant role.

Let us discuss this point in more detail. For 2D gases the transport and quantum times due to the interface roughness scattering are given by[18]

$$\frac{1}{\tau_{tr}} = \frac{m}{\pi\hbar^3}\int_0^\pi (1-\cos\Theta)\frac{U_q^2}{\varepsilon_q^2}d\Theta, \quad (8)$$

$$\frac{1}{\tau_q} = \frac{m}{\pi\hbar^3}\int_0^\pi \frac{U_q^2}{\varepsilon_q^2}d\Theta, \quad (9)$$

where Θ is the scattering angle. The dielectric function ε_q in the Thomas-Fermi approximation has the simple form $\varepsilon_q = 1+q_s/q$, where $q_s=me^2/2\pi\varepsilon_L\varepsilon_0\hbar^2$ is the Thomas-Fermi screening wave number, $\varepsilon_L, \varepsilon_0$ are the static dielectric constant of the semiconductor and the vacuum dielectric constant, respectively $q=2k_F\sin\Theta/2, k_F$ is the Fermi vector. The random potential due to the interface roughness is written as

$$U_q^2 = \pi\Delta^2\Lambda^2\left[\frac{e^2n_s}{4\varepsilon_L\varepsilon_0}\right]^2\exp(-q^2\Lambda^2/4). \quad (10)$$

We used the actual measured electron density n_s and parameters of the surface roughness Δ and Λ to calculate the transport and quantum scattering times in our samples. The results of the calculation for the sample KNU01 are shown in Fig. 3 as a function of the correlation length. We also indicate the experimentally measured τ_{tr} and τ_q. One can see that the calculations agree very well with the measured values.

Recently, it has been argued[19] that the quantum time τ_q deduced from the analysis of the Shubnikov–de Haas amplitude is much smaller than the quantum scattering time τ_{CR} determined from the width of the cyclotron resonance peak in the presence of small macroscopic inhomogeneity. Therefore, the time τ_q does not provide a reliable method to determine the scattering mechanism. We do not share this point of

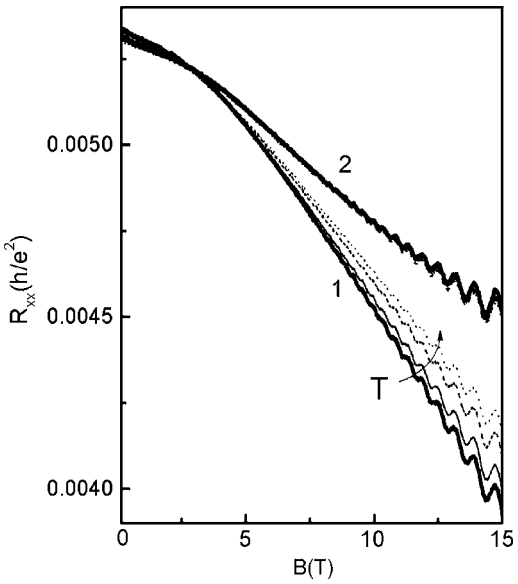

FIG. 4. (1) The magnetoresistance as a function of magnetic field for different temperatures (1.7, 3, 5, 10 K). (2) Magnetoresistance curves obtained after subtraction of the interaction corrections (see the text).

view: Of course macroscopic inhomogeneities can smooth SdH oscillations in low magnetic field, which leads to an increase of the slope in the Dingle plot. However, in this case the intercept of the Dingle straight line at $1/B=0$ results in $A \gg 1$ (see for example Ref. 20). A reliable evaluation of the quantum scattering time leads to a value of $A=1$. In our analysis we fit amplitude of the SdH oscillations with A=1; therefore, we believe that our evaluation of τ_q is correct.

According to all the developed arguments, we may conclude that the dominant scattering mechanism in our low-mobility, high-density 2D gas in $Al_xGa_{1-x}N/GaN$ heterostructures is the interface roughness scattering. In the presence of these strong scatterers the transport of 2D electrons should be more relevant to the Lorentz model,[5,9,11] which predicts a negative magnetoresistance.

IV. INTERACTION-INDUCED NEGATIVE MAGNETORESISTANCE IN A TWO-DIMENSIONAL DISORDERED SYSTEM

Figure 4 shows the longitudinal resistance R_{xx} of the sample KNU01 measured for different temperatures. A negative magnetoresistance can be observed before the onset of SdH oscillations. It is important to emphasize that, in addition to quasiclassical effects, quantum effects can also be a possible source of negative magnetoresistance. First, as we already mentioned, the weak localization results in a NMR at very low magnetic fields.[21] Second, electron-electron interactions induce a parabolic negative magnetoresistance[22,23] in stronger fields. Recently, the theory of the interaction-induced NMR has been extended to different regimes of the electron motion: in a short-range disorder potential (diffusive regime) and in a smooth potential (ballistic regime).[24] In weakly disordered system with high conductivity, $\sigma \gg g = e^2/h$, the standard theory of quantum corrections has been developed in the first order in $1/g$. In this case the conductivity of the system at $B=0$ can be written as[21]

$$\sigma_{xx} = \sigma_0 + \Delta\sigma_{WL} + \Delta\sigma_{int}. \tag{11}$$

The weak localization term is given by the equation

$$\Delta\sigma_{WL} = (pe^2/\pi h)\ln(k_B T\tau_{tr}/\hbar) + \text{const}, \tag{12}$$

where it is assumed that the phase-breaking time follows the power law, $\tau_\varphi \sim T^{-p}$. The quantum interaction corrections are given by

$$\Delta\sigma_{int} = (e^2/\pi h)\left\{3\left[1 - \frac{ln(1+F_0^\sigma)}{F_0^\sigma}\right] + 1\right\}\ln(k_B T\tau_{tr}/\hbar), \tag{13}$$

where F_0^σ is the Fermi-liquid constant. For weak interaction $(r_s \leqslant 1)$[25]

$$F_0^\sigma = -\frac{1}{2\pi}\frac{r_s}{\sqrt{2-r_s^2}}\ln\left(\frac{\sqrt{2}+\sqrt{2-r_s^2}}{\sqrt{2}-\sqrt{2-r_s^2}}\right), \tag{14}$$

where r_s is the dimensionless radius, which is equal to the ratio of the Coulomb and Fermi energies. In our samples we obtain $r_s \approx 0.74$, and, consequently $F_0^\sigma \approx -0.26$. It is well known that the weak localization corrections are suppressed by very small magnetic fields $B \gg \hbar/(2el_s^2) \sim 100$ mT. Moreover, the interaction correction to the conductivity is not sensitive to the magnetic field and the Hall conductivity is not affected by interaction in the diffusive regime. In this case the magnetoresistance derived by inverting the conductivity matrix, which is given by Eq. (2), has the form[22]

$$\rho_{xx}(B) - \rho_0 \simeq \frac{\Delta\sigma_{int}}{\sigma_0^2}[(\omega_c\tau_{tr})^2 - 1]. \tag{15}$$

This equation predicts a negative parabolic magnetoresistance with a logarithmic temperature dependence in the diffusive regime, when $k_B T\tau_{tr}/\hbar \ll 1$, followed by $T^{-1/2}$ dependence in the ballistic regime,[24] $k_B T\tau_{tr}/\hbar \gg 1$. In our samples the parameter $k_B T\tau_{tr}/\hbar$ is varied from 0.11 to 0.7 in the temperature range $T=1.7$–10 K.

This interaction-induced NMR has been observed in experiments for both the diffusive[26,27] and ballistic regimes[28,29] in $Al_xGa_{1-x}As/GaAs$ heterostructures.

Finally, we should mention the positive magnetoresistance arising from the Zeeman effect on the interaction correction.[21] The contribution of this effect has been measured in parallel magnetic field and is negligible in comparison with the studied negative magnetoresistance.

Let us proceed to the experimental results. One can see in Figs. 2 and 4 that the negative magnetoresistance shows a parabolic dependence followed by linear dependence in higher field. The parabolic magnetoresistance shows a weak temperature dependence that is attributed to the T dependence of the interaction-induced corrections. The following procedure allowed us to remove this contribution from the data. The resistance curves were converted into the conductance curves from which the interaction corrections [calculated using Eq. (13) with $F_0^\sigma \approx -0.26$] was then subtracted.

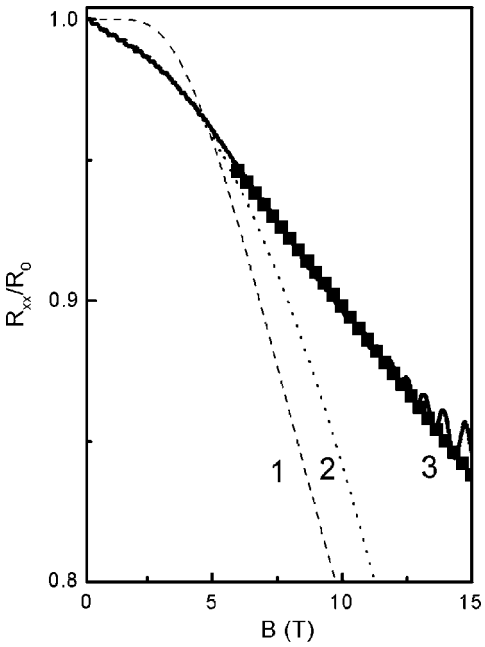

FIG. 5. The magnetoresistance obtained after subtraction interaction corrections from the total conductance as a function of magnetic field for $T=1.7$ K (solid curve). Dashes (curve 1): Eq. (3) for $\beta=0.4B(T)$; dots (curve 2): Eq. (5) for $\hbar\omega_0=13.8$ meV; squares: Eq. (4).

The conductance was then converted back into resistance curves and the result is plotted in Fig. 4. We see that all the magnetoresistance traces are collapsed into single temperature-independent curve. Therefore, one can conclude that, indeed, the data were cleaned of the interaction contribution and that the rest of the magnetoresistance has a classical (T-independent) origin. Note that the contribution of the classical effects is larger than the quantum contribution.

V. NEGATIVE MAGNETORESISTANCE IN A TWO-COMPONENT DISORDER SYSTEM

Figure 5 shows the temperature-independent part of the negative magnetoresistance obtained after processing the data as described above. We attribute this NMR to the non-Markovian dynamics of the electronic motion in the presence of strong scatterers (interface roughness) and smooth random potential (remote donors, microscopic density inhomogeneity) considered in Ref. 11. In low magnetic field such model predicts a parabolic negative MR, given by Eq. (5). Figure 5 shows that this equation almost perfectly describes the experimental curve with the parameter $\hbar\omega_0=13.8$ meV for $B<6$ T (curve 2). The parabolic dependence is valid for small NMR, when $\hbar\omega_c \ll \hbar\omega_0$. In our structure we find $\hbar\omega_c=0.52$ meV for $B=1$ T T; therefore the condition $\hbar\omega_c \sim \hbar\omega_0$ is satisfied at $B=23$ T. Another important energy, $\hbar\omega_\tau=2\pi\hbar/\tau_{tr}=h/\tau_{tr}=7.5$ meV, is responsible for pure Lorentz gas behavior. As has been shown in Ref. 11, for $\hbar\omega_\tau \ll \hbar\omega_0$, smooth potential does not affect the Lorentz gas results and the magnetoresistance is described by Eq. (3). In our case $\hbar\omega_\tau \sim \hbar\omega_0$; therefore, the two-component disorder model is valid. As we mentioned above, in a pure Lorentz gas scattered by hard disks, electrons are completely localized in magnetic fields $\omega_c > \omega_{perc}$ because the rosettelike cyclotron orbits fail to form infinite cluster and percolate through the sample. Two-dimensional electron systems with interface roughness scattering can be compared to a Lorentz gas where the correlation length plays the role of the radius of the disks. Assuming $l_s=1/(2Nd)\approx l_{tr,}$ we obtain $N=3\times10^{10}\text{cm}^{-2}$, which gives $\hbar\omega_{perc}=10.4$ meV. Finally, the energy $\hbar\omega_{cross}\approx\hbar\omega_0(\omega_\tau/\omega_0)^{1/3}\approx 12$ meV corresponds to the crossover from two-component disorder to pure Lorentz gas behavior. Comparing all characteristic frequencies, we conclude that in our situation we have $\omega_\tau < \omega_{perc} \sim \omega_{cross} \sim \omega_0$, which corresponds to the case considered in Ref. 11 when the Lorentz gas behavior is completely destroyed and Eq. (5) is valid in the whole range of magnetic field when $\omega_c \ll \omega_0$. At higher magnetic fields, when $\omega_c \sim \omega_0$ the NMR deviates from parabolic dependence and saturates, as can be seen in Fig. 1 of Ref. 11. This result is in agreement with our measurements. However, there are no analytical results in strong magnetic field, and numerical simulations would be necessary to explain our data. In this paper we compare our experimental curves to analytical results and, thus, focus on the low-field part of the negative magnetoresistance. From $\hbar\omega_0=13.8$ meV we obtain the ratio $l_L/l_s=2.8$. Assuming $l_s \sim l_{tr}=0.2$ μm, we find the mean free path due to the smooth disorder $l_L=0.56$ μm. Note that $\hbar\omega_0 \sim (l_s/l_L)^{1/4}$ and in practice the precision for determination of the ratio l_L/l_s is not very high.

When $l_L/l_s \to \infty$ the Lorentz gas behavior is recovered and the NMR is expressed by Eq. (3). We plot the theoretical curve (dashed line) in Fig. 5 for $\beta=0.4\times B(T)=\omega_c\tau_{tr}$. We also see that the Lorentz gas model does not explain negative parabolic dependence in the low-field part of the magnetoresistance. However, as we already mentioned in the Introduction, the Lorentz gas behavior in low magnetic field should be modified by non-Markovian memory effects resulting from specific backscattering processes.[8] Such model predicts a parabolic NMR in a very low magnetic field, which changes to a linear B dependence at higher fields. In principle, this theory could also explain our results. Figure 5 shows theoretical curves (squares) calculated using Eq. (4) in the range of magnetic fields where the linear approximation is valid. The theory[8] predicts that below $\beta=\omega_c\tau_{tr}\approx 0.05\beta_0$ the crossover to negative parabolic magnetoresistance should be observed. Experimentally, we observe that this crossover from the parabolic to linear behavior occurs at $B\approx 6$ T($\beta=2.4$); see Fig. 5. This leads to $\beta_0\approx 48$, which is not a realistic value since the model is valid for $\beta_0 \ll 1$. We found the same contradiction ($\beta_0 \gg 1$) when we tried to fit Eq. (4) to the negative parabolic magnetoresistance observed for $B<6$ T. Therefore, in spite of the good agreement with experiment in the intermediate region of the magnetic field, the model[8,9] does not explain the observed parabolic part of NMR. We believe that such discrepancy is due to the presence of the smooth disorder potential. Such potential strongly modifies the motion of electrons in the low magnetic field, but probably does not affect electrons trajectories in the field when $\omega_c\tau_{tr} \sim 1$.

VI. CONCLUSION

The 2D electrons in real systems move in a two-component disorder potential: a smooth random background and rare strong scatterers. Non-Markovian generalized solution of the Lorentz model predicts a negative magnetoresistance. We have compared this prediction to our observations of the NMR in a low-mobility, high-density 2D electron gas in an $Al_xGa_{1-x}N/GaN$ heterostructure and demonstrated that the magnetotransport in such system can be explained by memory effects within the classical approach. We believe that this analysis allowed us to deduce reliably the ratio between the mean free paths due to the smooth disorder and strong scatterers. Its is very difficult to obtain information about character of disorder in such structures from conventional Shubnikov–de Haas oscillations and zero-field mobility measurements only. We believe that our observation may emphasize the importance of the memory effects in transport properties which are beyond the Drude-Boltzmann approximation.

ACKNOWLEDGMENTS

This work is supported by Grant N R01-2003-000-10769-0 (2004) from Korea Science and Engineering Foundation, BK 21, INTAS (N 01-0014), RAS (programs LDS and PSSN), RFBR (N 05-02-16591), and NATO Linkage. Support of this work by FAPESP, CNPq (Brazilian agencies) and CNPq-CNRS is also acknowledged.

[1] A. V. Bobylev, Frank A. Maaø, Alex Hansen, and E. H. Hauge, Phys. Rev. Lett. **75**, 197 (1995).
[2] A. D. Mirlin, J. Wilke, F. Evers, D. G. Polyakov, and P. Wölfle, Phys. Rev. Lett. **83**, 2801 (1999).
[3] D. G. Polyakov, F. Evers, A. D. Mirlin, and P. Wölfle, Phys. Rev. B **64**, 205306 (2001).
[4] E. M. Baskin, L. N. Magarill, M. V. Entin, Sov. Phys. JETP **48**, 365 (1978), E. M. Baskin and M. V. Entin, Physica B, **249–251**, 805 (1998).
[5] A. Dmitriev, M. Dyakonov, and R. Jullien, Phys. Rev. B **64**, 233321 (2001).
[6] G. M. Gusev, P. Basmaji, Z. D. Kvon, L. V. Litvin, Yu. V. Nastaushev, and A. I. Toropov, Surf. Sci. **305**, 443 (1994).
[7] G. M. Gusev, P. Basmaji, Z. D. Kvon, L. V. Litvin, Yu. V. Nastaushev, and A. I. Toropov, J. Phys.: Condens. Matter **6**, 73 (1994).
[8] A. Dmitriev, M. Dyakonov, and R. Jullien, Phys. Rev. Lett. **89**, 266804 (2002).
[9] V. V. Cheianov, A. P. Dmitriev, and V. Yu. Kachorovskii, Phys. Rev. B **68**, 201304(R) (2003).
[10] N. M. Sotomayor, G. M. Gusev, J. R. Leite, A. A. Bykov, A. K. Kalagin, V. M. Kudryashev, and A. I. Toropov, Phys. Rev. B **70**, 235326 (2004).
[11] A. D. Mirlin, D. G. Polyakov, F. Evers, and P. Wolfle, Phys. Rev. Lett. **87**, 126805 (2001).
[12] A. A. Bykov, A. K. Bakarov, A. V. Goran, N. D. Aksenova, A. V. Popova, and A. I. Toropov, JETP Lett. **78**, 165 (2003).
[13] S. Nakamura, M. Senoh, N. Iwasa, S. Nagahama, T. Yamada, and T. Mukai, Jpn. J. Appl. Phys., Part 2 **36**, L1568 (1997).
[14] M. J. Manfra, L. N. Pfeiffer, K. N. West, H. L. Stormer, K. W. Baldwin, J. W. P. Hsu, and D. V. Lang, Appl. Phys. Lett. **77**, 2888 (2000).
[15] T. Wang, J. Bai, S. Sakai, Y. Ohno, and H. Ohno, Appl. Phys. Lett. **76**, 2737 (2000).
[16] J. R. Juang, Tsai-Yu Huang, Tse-Ming Chen, Ming-Gu Ling, Gil-Ho Kim, Y. Lee, C.-T. Liang, D. R. Hang, Y. F. Chen, and Jen-Inn Chyi, J. Appl. Phys. **94**, 3181 (2003).
[17] H. Tang, J. B. Webb, P. Coleridge, J. A. Bardwell, C. H. Ko, Y. K. Su, S. J. Chang, Phys. Rev. B **66**, 245305 (2002).
[18] A. Gold, Phys. Rev. B **38**, 10798 (1988).
[19] S. Syed, M. J. Manfra, Y. J. Wang, R. J. Molnar, and H. L. Stormer, Appl. Phys. Lett. **84**, 1507 (2004).
[20] P. T. Coleridge, Phys. Rev. B **44**, 3793 (1991).
[21] P. A. Lee, and T. V. Ramakrishnan, Rev. Mod. Phys. **57**, 287 (1985).
[22] A. Houghton, J. R. Senna, and S. C. Ying, Phys. Rev. B **25**, 2196 (1982).
[23] S. M. Girvin, M. Jonson, and P. A. Lee, Phys. Rev. B **26**, 1651 (1982).
[24] I. V. Gornyi and A. D. Mirlin, Phys. Rev. Lett. **90**, 076801 (2003).
[25] G. Zala, B. N. Narozhny, and I. L. Aleiner, Phys. Rev. B **64**, 214204 (2001).
[26] G. M. Minkov, O. E. Rut, A. V. Germanenko, A. A. Sherstobitov, V. I. Shashkin, O. I. Khrykin, and V. M. Daniltsev, Phys. Rev. B **64**, 235327 (2001).
[27] V. Renard, Z. D. Kvon, O. Estibals, J. C. Portal, A. I. Toropov, A. K. Bakarov, and M. N. Kostrikin, Physica E (Amsterdam) **22**, 328 (2004).
[28] M. A. Paalanen, D. C. Tsui, and J. C. M. Hwang, Phys. Rev. Lett. **51**, 2226 (1983).
[29] L. Li, Y. Y. Proskuryakov, A. K. Savchenko, E. H. Linfield, and D. A. Ritchie, Phys. Rev. Lett. **90**, 076802 (2003).